Proc. Natl. Acad. Sci. USA
Vol. 79, pp. 4868–4872, August 1982
Biochemistry

Refined crystal structure of the molecular complex of *Streptomyces griseus* protease B, a serine protease, with the third domain of the ovomucoid inhibitor from turkey

(tetrahedral intermediate/Michaelis complex/pancreatic trypsin inhibitor)

MASAO FUJINAGA*, RANDY J. READ*, ANITA SIELECKI*, WOJCIECH ARDELT†, MICHAEL LASKOWSKI, JR.†, AND MICHAEL N. G. JAMES*‡

*Medical Research Council of Canada Group in Protein Structure and Function, Department of Biochemistry, University of Alberta, Edmonton, Alberta, Canada, T6G 2H7; and †Department of Chemistry, Purdue University, West Lafayette, Indiana 47907

Communicated by John T. Edsall, May 3, 1982

ABSTRACT **We have determined the crystal structure of the molecular complex between *Streptomyces griseus* protease B (SGPB), a bacterial serine protease, and the third domain of the ovomucoid inhibitor from turkey. Restrained-parameter least-squares refinement of the structure with the 1.8-Å intensity data set has resulted in an *R* factor of 0.125. The carbonyl carbon atom of the reactive bond between Leu-18 and Glu-19 in the inhibitor lies at a distance of 2.71 Å from the O^{γ} atom of the nucleophilic Ser-195 in SGPB; this distance is 0.5 Å shorter than a normal van der Waals contact. Unlike the reactive bond in the pancreatic trypsin inhibitor complexed with bovine trypsin, the Leu—Glu bond of the ovomucoid inhibitor is not distorted from planarity towards a pyramidal configuration.**

Protein inhibitors of the serine proteases have been grouped into 10 separate families (1). The ovomucoids from birds are homologous to the pancreatic secretory trypsin inhibitor (Kazal) (2) but consist of three homologous tandem domains of approximately 60 residues each. The crystal structure of the third domain from the ovomucoid inhibitor of Japanese quail has been reported at 2.8-Å resolution (3) and is being refined at 1.9-Å resolution. The homologous third domain from turkey ovomucoid inhibitor (OMTKY3; 56 amino acids) inhibits those serine proteases that have a chymotryptic specificity, and we have chosen this molecule for our crystallographic studies on serine proteases.

Streptomyces griseus protease B (SGPB) is a bacterial serine protease of M_r 18,500, which has a P_1 specificity[§] for Phe, Tyr, and Leu residues (5, 6). The crystal structure of SGPB, originally reported in 1975 (7), has recently been refined at 1.7-Å resolution to a conventional crystallographic *R* factor of 0.149 ($R = \Sigma||F_o| - |F_c||/\Sigma|F_o|$, in which $|F_o|$ and $|F_c|$ are the measured and computed structure-factor amplitudes, respectively; unpublished results). Tripeptide chloromethylketone inhibitor complexes of SGPB have identified enzyme binding sites S_1 to S_4 for oligopeptide substrates (8). It has been demonstrated that OMTKY3 forms a stoichiometric complex with SGPB (unpublished data).

Protein inhibitors of serine proteases have a common inhibitory mechanism (1). They bind very tightly to the active sites of their cognate enzymes but their reactive bonds (P_1—P_1') are hydrolyzed at very slow rates. The present structure of the SGPB·OMTKY3 complex suggests some reasons for this behavior.

The molecular structures of three protein inhibitor–protease complexes have been determined crystallographically: the Kunitz pancreatic trypsin inhibitor (PTI) with bovine trypsin (9, 10), the soybean trypsin inhibitor (STI) with porcine trypsin (11), and *Streptomyces* subtilisin inhibitor (SSI) with subtilisin BPN′ (12). Of these, only the trypsin·PTI complex has been done at sufficiently high resolution and the structure refined so that reliable comparisons of the molecular geometry in the region of the scissile bond can be made with the present complex.

The amino acid sequence of OMTKY3 (13) is shown in Fig. 1*a*. Our numbering origin corresponds to residue 131 of the complete ovomucoid. The reactive bond is between Leu-18 and Glu-19 (Leu-18I-Glu-19I; residues of the inhibitor have an I after the sequence number to distinguish them from those of SGPB).

MATERIALS AND METHODS

Purification of SGPB followed the procedure of Jurášek *et al.* (16); the method of purification of OMTKY3 is similar to that published by Bogard *et al.* (17). Crystallization of the SGPB·OMTKY3 complex was achieved by vapor diffusion from 10-μl droplets of a 1:1.5 molar ratio of enzyme and inhibitor in 0.75 M (K/Na)H_2PO_4 at pH 6.3. The first tiny crystals appeared after 4 months. Larger crystals, suitable for x-ray diffraction studies, were prepared by careful seeding of the microcrystals into freshly prepared solutions (vapor diffusion droplets) of inhibitor and enzyme. The initial structure solution was done on a 2.8-Å resolution intensity data set from a small crystal. Subsequently, 1.8-Å resolution data (18,100 unique reflections) were collected from a second, larger crystal that measured 0.84 × 0.75 × 0.15 mm. This latter data set was used for the refinement procedure. The x-ray intensity data were collected on a Nonius CAD4 diffractometer with the full ω-scan provision. Seventeen reflections in the range $16° < 2\theta < 31°$ were used to determine the crystal unit-cell parameters of $a = 45.35(4)$ Å, $b = 54.52(5)$ Å, $c = 45.65(4)$ Å, and $\beta = 119.2(1)°$ (numbers in parentheses are estimated SD). The space group is $P2_1$, with one molecule of the complex per asymmetric unit. Corrections were made for

The publication costs of this article were defrayed in part by page charge payment. This article must therefore be hereby marked "*advertisement*" in accordance with 18 U. S. C. §1734 solely to indicate this fact.

Abbreviations: SGPA, *Streptomyces griseus* protease A; SGPB, *Streptomyces griseus* protease B; OMTKY3, third domain of the turkey ovomucoid inhibitor; PTI, pancreatic trypsin inhibitor; SSI, *Streptomyces* subtilisin inhibitor; STI, soybean trypsin inhibitor.

‡To whom reprint requests should be addressed.

§The nomenclature introduced by Schechter and Berger (4) is used to facilitate discussion about the interactions between a protease and bound peptides. Amino acid residues of substrates are numbered P_1, P_2, P_3, etc., towards the NH_2-terminal direction and P_1', P_2', etc., in the COOH-terminal direction from the scissile bond. The complementary subsites of the enzyme binding region are numbered S_1, S_2, and S_1', S_2', etc.

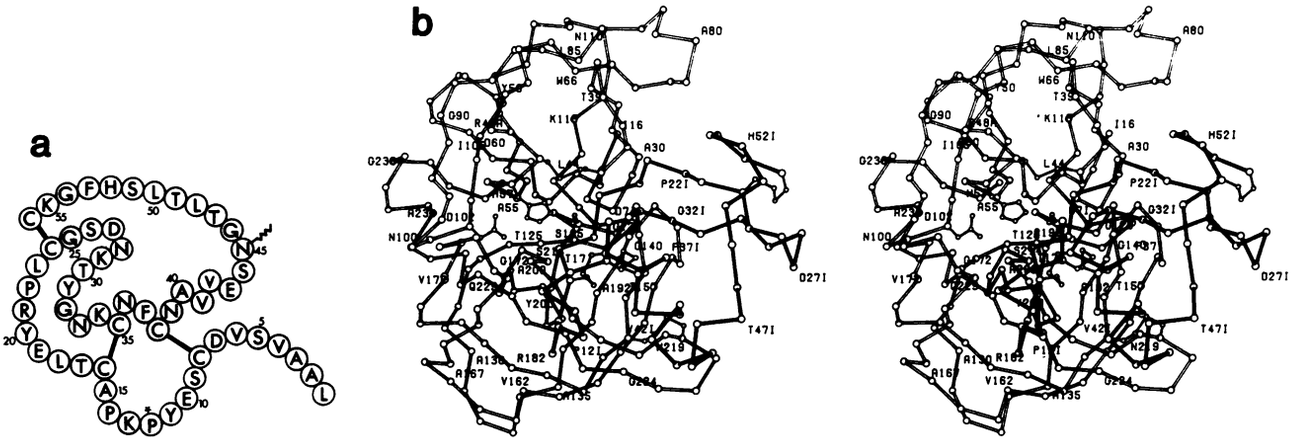

FIG. 1. (*a*) The amino acid sequence (one letter code) of the third domain of turkey ovomucoid inhibitor, OMTKY3 (13). The asparagine at position 45, marked by the sawtooth, is the site of glycosylation in the intact inhibitor. The carbohydrate-free domain was used in this work. The asterisk on Pro-12I indicates a *cis* configuration for that peptide (Y-11I—P-12I). The scissile peptide bond is between Leu-18I and Glu-19I. (*b*) An α-carbon representation of the molecular complex between SGPB (open bonds) and OMTKY3 (filled bonds). Every fifth amino acid residue in each molecule is labeled with the residue type and sequence number. The numbering of SGPB is that of chymotrypsinogen A (14) as previously reported (15). The numbering of OMTKY3 is given in *a* with an I after the residue number.

absorption (18) (maximum applied factor, 1.61), decay (19) (maximum, 18% overall), and Lorentz polarization. The absolute scale (7.1) and mean isotropic thermal vibration factor, *B* (13.1 Å^2), were determined by the program ORESTES (20).

The initial phases for the structure of the complex were determined by the technique of molecular replacement, by using as the search model the crystal structure of native SGPB, which had been refined at the time of this work to a conventional *R* factor of 0.177 for the 1.7-Å resolution data. The rotational parameters required to orient the search model correctly in the unit cell of the complex were determined by using the fast rotation function (21). The translation problem was overcome with an *R*-factor search. The minimum in the array of *R* factors was 0.35 (calculated in the 5-Å to 4-Å shell), which was 8 SD lower than the average of 0.44.

The appropriately rotated and translated atomic coordinates of the SGPB molecule were used to compute a difference electron density map (coefficients $|F_o| - |F_c|$, phases α_c) and an F_o map. All interpretations and model fitting of the unknown inhibitor molecule were done with the MMS-X interactive vector graphics system (22) at the University of Alberta. The macromolecular modeling system, M3, of C. Broughton (23) was used for all manipulations.

A total of 50 amino acid residues of the OMTKY3 molecule (out of 56 residues) could be located. The NH_2-terminal hexapeptide Leu-Ala-Ala-Val-Ser-Val was not visible on the 2.8-Å electron density map. The density for Asp-7I, Ser-9I, and Glu-10I was very weak but a model was eventually derived for these residues. Thus, least-squares refinement was initiated with the rotated–translated SGPB coordinates and the newly derived structure for 50 of the residues of the ovomucoid inhibitor. A total of 46 cycles of restrained-parameter least-squares refinement (24) has reduced the agreement factor, *R*, from 0.31 (8.0- to 2.8-Å resolution) to 0.125 (8.0- to 1.8-Å resolution). The resulting rms deviations from expected stereochemical parameters are: 0.016 Å for the 1,728 covalent bonds; 0.038 Å for the 2,347 interbond angle distances; and 0.019 Å from the 300 planar groups of the complex. The rms deviation of the 233 peptide bond torsional angles is 3.5°. So far, 142 water molecules have been included in the structural model; these solvent sites range in occupancy from 0.43 to 1.00.

RESULTS AND DISCUSSION

Description of the Structure. Serine proteases are characterized by two similarly folded domains, each comprising approximately one-half of the residues of the molecule. The active site residues Asp-102, His-57, and Ser-195 are located at the interdomain junction, which also forms the substrate binding sites (8). We have shown that the bacterial enzymes have extensive three-dimensional structural homology with the pancreatic enzymes trypsin, chymotrypsin, and elastase (7, 15). Therefore, binding interactions that we observe here for the Kazal inhibitors with SGPB are sure to resemble those with the pancreatic enzymes.

The overall view of the manner in which the ovomucoid inhibitor binds to SGPB is shown in Fig. 1*b*. It can be seen that the polypeptide chain of OMTKY3 from Lys-13I to Arg-21I spans the active site of SGPB in such a way that the reactive bond, Leu-18I—Glu-19I, is brought into close proximity to the active site residues. Hydrogen bonding and interactions with two predominantly hydrophobic sites on the surface of the SGPB molecule—the S_1 site that accommodates the P_1 leucyl side chain and the S_2 site that accommodates the P_2 threonyl side chain—stabilize the complex. This mode of binding is very similar to the tetrapeptide product and aldehyde binding we have observed with the homologous bacterial enzyme *Streptomyces griseus* protease A (SGPA) (25, 26).

The third domain of the turkey ovomucoid inhibitor may be described, overall, as a wedge-shaped disc. The present independent structure determination of the Kazal fold shows that the domain from turkey is extremely similar to the molecular structure of the homologous domain of the Japanese quail ovomucoid inhibitor (3). Such an observation is not surprising as the sequences of these two domains differ only at six positions (three of which, at positions 17I, 18I, and 19I, bracket and include the main specificity residue for the inhibitor's cognate enzyme).

Approximately 50% of the residues of OMTKY3 form two secondary structural units. Thirteen (Asn-33I to Asn-45I) are in an α-helical conformation (see Fig. 1*b*). Eleven residues (Leu-23I to Ser-26I, Asp-27I to Tyr-31I, and Ser-51I—His-52I) form a small antiparallel β-sheet that contains one reverse turn of type I (Gly-25I—Asn-28I). The segments of polypeptide chain from Cys-8I to Cys-16I and from Cys-16I to Pro-22I adopt

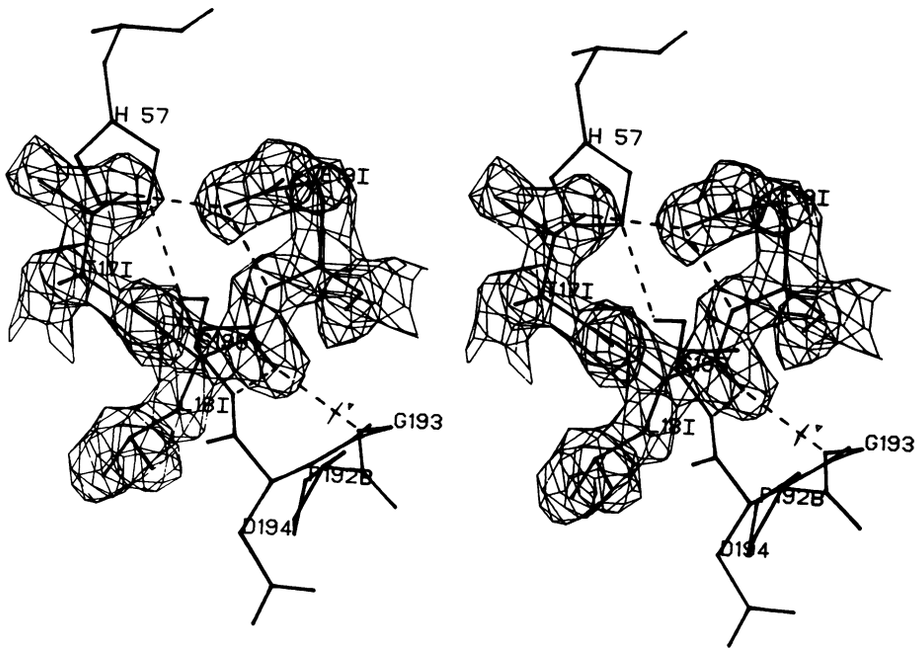

FIG. 2. A stereo representation of the electron density of the three residues Thr-17I, Leu-18I, and Glu-19I of OMTKY3 bound to the active site of SGPB. The electron density distribution is that of a $2F_o - F_c$, α_c map computed at an R factor of 0.125 from the 12,155 statistically significant structure factor amplitudes measured in the 8.0- to 1.8-Å resolution shell. The contour level represented here is +0.50 electron per Å^3. The amino acids His-57, Pro-192B, Gly-193, Asp-194, and Ser-195 of SGPB are shown without their electron density. The electron density shown for the peptide bond Leu-18I—Glu-19I is consistent with the inhibitor model having a planar peptide bond (ω = 175°). There is little, if any, pyramidalization of the carbonyl carbon atom of the scissile bond. Hydrogen bonding is denoted by dashed lines between atoms.

an extended conformation, with the two disulfide bridges (Cys-8I—Cys-38I and Cys-16I—Cys-35I) providing the main interactions with the more highly organized core of the molecule. The first six residues in OMTKY3 are fully disordered in the crystals of the complex (there is no electron density for residues Leu-1I—Val-6I).

Reactive Site Geometry. Fig. 2 shows a close-up view of the vicinity of the reactive bond Leu-18I—Glu-19I of the inhibitor in the active site of SGPB. An ORTEP (27) drawing of a larger region of this active site is presented in Fig. 3. There are 106 intermolecular van der Waals contact and hydrogen bond distances less than 4.0 Å. Relatively few residues, 17 of 185 in SGPB and 11 of 56 (50 structurally determined) in the ovomucoid inhibitor third domain, are involved in the interaction. The residues most important for the binding are: Thr-17I, Leu-18I, and Tyr-20I in OMTKY3 and Arg-41, His-57, Tyr-171, Pro-192B, Ser-195, and Gly-216 in SGPB.

The torsional angle ω at the scissile bond (C^{α}_{18I}—CO—N—C^{α}_{19I}) is 175°, not significantly different from the expected value of 180°. Moreover, this angle remained essentially unchanged (173°) when all planar restraints on atoms of the inhibitor were released during several cycles of least-squares refinement at an intermediate stage of the refinement. Additionally, if pyramidalization of the carbonyl carbon atom of this peptide had occurred, the θ^4 angle (the out-of-plane bend angle, plane defined by C^{α}, C, N) would be −54°; θ^4 for the carbonyl oxygen atom of Leu-18I in OMTKY3 is −5°. Fig. 2 shows the corresponding electron density distribution of the atoms comprising this planar peptide bond.

This result is in marked contrast with the reported geometry of the analogous peptide bond Lys-15I—Ala-16I in the trypsin·PTI complex, the anhydrotrypsin·PTI complex, and the trypsinogen·PTI·Ile-Val ternary complex (10). In each of these complexes the θ^4 angle for the carbonyl oxygen of Lys-15I in PTI is −34°. However, the authors acknowledge that this apparent pyramidal distortion is much larger than would be expected from the equation derived by Bürgi *et al.* (28), which predicts an out-of-plane displacement for the carbonyl carbon of less than 0.09 Å when the nucleophile approach distance is ≈2.7 Å. It should be pointed out that such a displacement would be close to the limit of detection allowed by the accuracy of fully refined protein coordinates. The nonbonded contact distance from O^{γ} of Ser-195 (the incipient nucleophile) to the carbonyl carbon atom of the potential scissile bond is 2.6 Å in the trypsin·PTI complex and 2.7 Å in the SGPB·OMTKY3 complex. The conformations of the polypeptide chains from P_3 to P_2' in the refined structures of the SGPB·OMTKY3 and the trypsin·PTI complexes are similar. The sequences of the two inhibitors are different, which certainly accounts for some of the observed conformational differences. In spite of these, the five α-carbon atoms for the two inhibitors (residues P_3—P_2') agree in position to within 0.82 Å (rms deviation, 0.52 Å) when

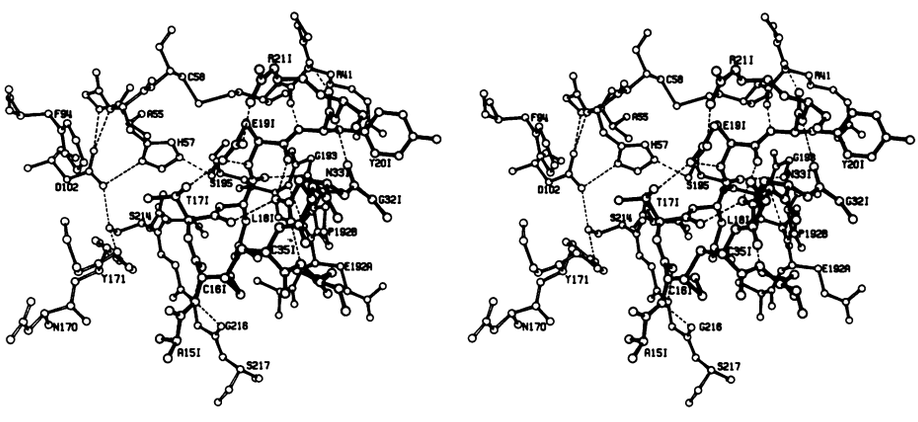

FIG. 3. An ORTEP (27) plot of the contact region in the molecular complex of SGPB·OMTKY3 (Lys-13I, as well as the side chain of Lys-34I, have been omitted for clarity). Residues of SGPB are displayed with open bonds, whereas residues of the inhibitor are represented by filled bonds between atoms. Hydrogen bonds (see Table 1 for details) are denoted by dashed lines. The close contact (attractive interaction) from Ser-195 O^{γ} to the carbonyl carbon atom of Leu-18I is 2.71 Å.

the two complexes are rotated and translated to a common orientation via a least-squares procedure (29).

Table 1 summarizes the hydrogen-bonding interactions that occur at the interface between enzyme and inhibitor. There are seven hydrogen bonds that stabilize the complex. Two are made in an antiparallel fashion from Cys-16I to the main chain of SGPB at Gly-216. In a similar way, Tyr-20I forms two hydrogen bonds to the main chain of SGPB at Arg-41. (In the trypsin·PTI complex, conformational differences in both enzyme and inhibitor limit these four possible hydrogen-bonding interactions to two.) A fifth hydrogen bond is from the N^{ζ} of Lys-13I to the carbonyl oxygen of Tyr-171. This interaction is unique to the bacterial proteases, because the methionine loop (residues 168–182) has a very different conformation in the bacterial proteases compared with the pancreatic enzymes (7, 15).

The carbonyl oxygen of Leu-18I lies close to the oxyanion binding site of SGPB and is the recipient of the two remaining hydrogen bonds (Fig. 3). The one to Gly-193 N—H is quite strong, whereas the long distance of 3.10 Å to Ser-195 N—H indicates a relatively weak bond. The equivalent hydrogen bonds in the trypsin·PTI complex have been invoked to explain the apparent pyramidalization of the carbonyl carbon atom of the reactive bond (Lys-15I). Because these hydrogen bonds are of similar lengths to the ones in the refined SGPB·OMTKY3 complex, which has a planar reactive peptide, it is unlikely that they are the cause of distortion.

Restraints to the Formation of the Tetrahedral Intermediate. Apart from hydrogen bonds, the only intermolecular contacts in the complex that are significantly shorter than the sum of the van der Waals radii involve O^{γ} of Ser-195. One might have expected this atom to move away from these contacts because there is only a small barrier to the rotation of the C^{α}—C^{β} bond in Ser-195, except for the possible disruption of the hydrogen bond from O^{γ} to $N^{\varepsilon 2}$ of His-57. [This hydrogen bond, which is weak (3.03 Å) in the native enzyme, becomes strong (2.55 Å) upon formation of the complex.] We are thus led to conclude that the short distance between O^{γ}, and the carbonyl carbon of Leu-18I represents an attractive interaction but not a covalent bond.

The observed geometry at the reactive site is consistent with an arrested nucleophilic attack of Ser-195 O^{γ} on the carbonyl carbon atom of Leu-18I. However, the structure of the enzyme inhibitor complex has several restricting steric interactions that prevent the completion of this attack to form the tetrahedral intermediate.

Conformational inflexibility in the complex would contribute to a reduced reaction rate. Analysis of the atomic *B* factors resulting from the crystallographic refinement can support this concept. The average *B* factor (thermal motion parameter) for all main-chain atoms of the inhibitor is 14.7 $Å^2$, whereas those for the main-chain atoms of residues P_3 to P_3' are much smaller and range from 5.4 to 7.9 $Å^2$. The atoms comprising the reactive peptide bond between Leu-18I and Glu-19I have the lowest *B* factors in the molecule, indicating the least flexibility.

Table 1. Inter- and intramolecular hydrogen bonding at the enzyme–inhibitor interface

	Donor			Acceptor	Distance, Å
P_6	Lys-13I	N^{ζ}·····O=C		Tyr-171	2.92
P_3	Cys-16I	N—H·····O=C		Gly-216	2.99
	Gly-216	N—H·····O=C	P_3	Cys-16I	2.92
	Gly-193	N—H·····O=C	P_1	Leu-18I	2.60
	Ser-195	N—H·····O=C	P_1	Leu-18I	3.10
P_2'	Tyr-20I	N—H·····O=C		Arg-41	2.84
	Arg-41	N—H·····O=C	P_2'	Tyr-20I	3.15
P_2	Thr-17I	$O^{\gamma 1}$—H·····$O^{\varepsilon 1}$—C^{δ}	P_1'	Glu-19I	2.54
P_{15}'	Asn-33I	$N^{\delta 2}$—H·····O=C	P_2	Thr-17I	2.98
P_{15}'	Asn-33I	$N^{\delta 2}$—H·····O=C	P_1'	Glu-19I	2.93
P_1'	Glu-19I	N—H·····$O^{\varepsilon 1}$—C^{δ}	P_1'	Glu-19I	2.93

Conversion of an enzyme–substrate complex into a covalently attached tetrahedral intermediate involves small movements both of the enzyme and of the substrate. These relative motions have been described for the related serine protease, SGPA (25), in complex with the covalent adduct to Ac-Pro-Ala-Pro-Phe-H, an aldehyde (26). Although the aldehyde oxygen atom is protonated, that inhibitor provides us with a reasonable analogue of the tetrahedral intermediate, because in that structure the hemiacetal bond to the O^{γ} atom of Ser-195 of SGPA is undoubtedly tetrahedral in nature, with a covalent bond length of 1.73 Å (26). A comparison of the active site of SGPA plus the covalently attached tetrapeptide aldehyde with the active site of SGPB and the bound OMTKY3 is shown in Fig. 4. This figure suggests the molecular movements that would be required to convert the enzyme–inhibitor complex (the reactive peptide of OMTKY3) into the corresponding tetrahedral intermediate. In forming the covalent bond to the carbonyl carbon of Leu-18I, O^{γ} of Ser-195 has to move approximately 0.9 Å (Fig. 4) and the carbonyl carbon of the inhibitor has to move ≈1.4 Å. These two movements are large and would require the concerted changes of many main-chain ϕ, ψ angles. However, there are several specific tertiary structural interactions that hinder these required motions.

Two hydrogen bonds restrain the movement of the polypeptide chain in the region of the reactive bond of the inhibitor.

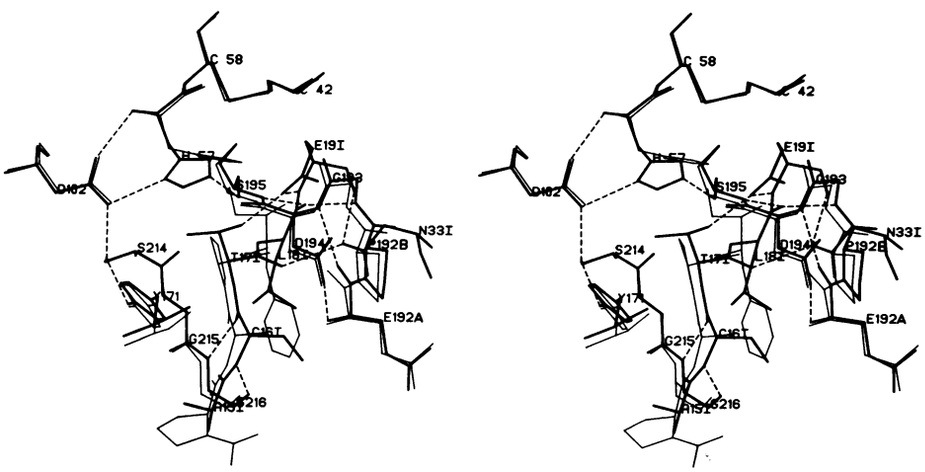

FIG. 4. A comparison of the active site region of a structure of a tetrahedral intermediate (thin lines) with the SGPB·OMTKY3 complex (thick lines; dashed lines for hydrogen bonds). The model structure is that of the tetrapeptide aldehyde Ac-Pro-Ala-Pro-Phe-H covalently attached to SGPA through a hemiacetal bond (26). The two structures were superimposed by a least-squares procedure that used main chain atoms of equivalent residues (560 atoms). The rms deviation for these atoms is 0.40 Å. The large movement necessary for the atoms in OMTKY3 to achieve the formation of the tetrahedral intermediate is evident.

Asn-33I, a strongly conserved residue in the ovomucoid inhibitors, donates a hydrogen bond to the carbonyl oxygen atom of Thr-17I and a second one to the carbonyl oxygen atom of Glu-19I. The required movement of the carbonyl carbon atom of Leu-18I towards O^{γ} of Ser-195 (see Fig. 4) is opposed by these two hydrogen bonds from $N^{\delta 2}$ of Asn-33I.

Another interaction that could contribute to an increase in the activation energy barrier to the formation of the tetrahedral intermediate in OMTKY3 is the hydrogen bond from the N—H of Glu-19I to the side chain carboxylate $O^{\epsilon 1}$ of the same residue (Table 1). This is an unusual conformation for a glutamate side chain (Fig. 3) that is stabilized further by a hydrogen bond from $O^{\gamma 1}$ of Thr-17I. A similar hydrogen-bonded interaction is seen in the OMJPQ3 structure (3), in which the P_1' residue is an aspartic acid but the hydrogen bond from O^{δ} of the carboxylate to the N—H of the peptide is also formed (2.78 Å). Pyramidalization of the nitrogen atom is concerted with the formation of the tetrahedral intermediate.

The theory of stereoelectronic control of amide hydrolysis (30) indicates that, for the breakdown of a tetrahedral intermediate, the lone pair orbitals of the heteroatoms must be oriented antiperiplanar to the bond being broken. By the principle of microscopic reversibility, the lone pair orbitals developing on the heteroatoms during the formation of a tetrahedral intermediate must be antiperiplanar to the new bond. As a result, the proton on the nitrogen must point initially towards the imidazole of His-57 (31, 32). Such a reorientation of the hydrogen bond donor, coupled with its movement towards Ser-195, would weaken and possibly disrupt the hydrogen bond involving the P_1' residue, thus increasing the activation energy barrier.

It is of great interest to note that in PTI a hydrogen bond involving the scissile bond N—H of the P_1' residue, Ala-16I, is also present. The acceptor atom in the PTI case is the carbonyl oxygen of the main chain of Gly-36I which is in a β-sheet structure (Gly-36I—Cys-38I is antiparallel to Lys-15I—Ala-16I) (10). The presence of this hydrogen bond in the case of PTI should also contribute to the reduced rate of formation of the tetrahedral intermediate in the manner discussed above. The situation is less clear in the case of *Streptomyces* subtilisin inhibitor (SSI) with subtilisin BPN′ (12) but the native 2.6-Å resolution structure of SSI indicates that the side chain of Asn-99I could form a hydrogen bond to the leaving group N—H of Val-75I. Higher resolution for that structural study would be required to resolve this problem.

The molecular complex SGPB·OMTKY3 refined at 1.8-Å resolution has provided new data relevant to the hydrolytic mechanism of serine proteases. The inhibitor binds in a manner superficially similar to that of a good substrate, but several key intramolecular interactions hinder a sufficiently close approach of the scissile bond to the nucleophilic serine thereby inhibiting the formation of the tetrahedral intermediate.

Koto Hayakawa grew the crystals of this molecular complex. The staff at the computer center at the University of Alberta have been very helpful during this study. M.F. and R.J.R. are holders of Medical Research Council of Canada Studentships and Alberta Heritage Fund for Medical Research Allowances. The crystal structure analysis at the University of Alberta was funded by grants to the Medical Research Council Group in Protein Structure and Function by the Medical Research Council of Canada. The isolation and purification of OMTKY3 at Purdue was supported by National Institutes of Health Grant GM 10831.

1. Laskowski, M., Jr., & Kato, I. (1980) *Annu. Rev. Biochem.* **49,** 593–626.
2. Kazal, L. A., Spicer, D. S. & Brahinsky, R. A. (1948) *J. Am. Chem. Soc.* **70,** 3034–3040.
3. Weber, E., Papamokos, E., Bode, W., Huber, R., Kato, I. & Laskowski, M., Jr. (1981) *J. Mol. Biol.* **149,** 109–123.
4. Schechter, I. & Berger, A. (1967) *Biochem. Biophys. Res. Commun.* **27,** 157–162.
5. Jurášek, L., Carpenter, M. R., Smillie, L. B., Gertler, A., Levy, S. & Ericsson, L. H. (1974) *Biochem. Biophys. Res. Commun.* **61,** 1095–1100.
6. Bauer, C.-A. (1978) *Biochemistry* **17,** 375–380.
7. Delbaere, L. T. J., Hutcheon, W. L. B., James, M. N. G. & Thiessen, W. E. (1975) *Nature (London)* **257,** 758–763.
8. James, M. N. G., Brayer, G. D., Delbaere, L. T. J., Sielecki, A. R. & Gertler, A. (1980) *J. Mol. Biol.* **139,** 423–438.
9. Huber, R., Kukla, D., Bode, W., Schwager, P., Bartels, K., Deisenhofer, J. & Steigemann, W. (1974) *J. Mol. Biol.* **89,** 73–101.
10. Huber, R. & Bode, W. (1978) *Acc. Chem. Res.* **11,** 114–122.
11. Sweet, R. M., Wright, H. T., Janin, J., Chothia, C. H. & Blow, D. M. (1974) *Biochemistry* **13,** 4212–4228.
12. Hirono, S., Nakamura, K. T., Iitaka, Y. & Mitsui, Y. (1979) *J. Mol. Biol.* **131,** 855–869.
13. Kato, I., Kohr, W. J. & Laskowski, M., Jr. (1978) in *Regulatory Proteolytic Enzymes and their Inhibitors,* 11th FEBS Meeting, eds. Magnusson, S., Ottesen, M., Foltmann, B., Danø, K. & Neurath, H. (Pergamon, Oxford), Vol. 47, pp. 197–206.
14. Hartley, B. S. & Kauffman, D. L. (1966) *Biochem. J.* **101,** 229–231.
15. James, M. N. G., Delbaere, L. T. J. & Brayer, G. D. (1978) *Can. J. Biochem.* **56,** 396–402.
16. Jurášek, L., Johnson, P., Olafson, R. W. & Smillie, L. B. (1971) *Can. J. Biochem.* **49,** 1195–1201.
17. Bogard, W. C., Kato, I. & Laskowski, M., Jr. (1980) *J. Biol. Chem.* **255,** 6569–6574.
18. North, A. C. T., Phillips, D. C. & Mathews, F. S. (1968) *Acta Crystallogr. Sect. A* **24,** 351–359.
19. Hendrickson, W. A. (1976) *J. Mol. Biol.* **106,** 889–893.
20. Thiessen, W. E. & Levy, H. A. (1973) *J. Appl. Crystallogr.* **6,** 309.
21. Crowther, R. A. (1973) in *The Molecular Replacement Method,* International Science Review 13, ed. Rossmann, M. G. (Gordon & Breach, New York), pp. 173–178.
22. Barry, C. D., Molnar, C. E. & Rosenberger, F. U. (1976) *Technical Memo* 229, Computer Systems Lab., Washington University, St. Louis, MO.
23. Sielecki, A. R., James, M. N. G. & Broughton, C. G. (1982) in *Computational Crystallography,* ed. Sayre, D. (Oxford Univ. Press, Oxford), pp. 409–419.
24. Hendrickson, W. A. & Konnert, J. H. (1980) in *Biomolecular Structure, Function, Conformation and Evolution,* ed. Srinivasan, R. (Pergamon, Oxford), Vol. 1, pp. 43–57.
25. Sielecki, A. R., Hendrickson, W. A., Broughton, C. G., Delbaere, L. T. J., Brayer, G. D. & James, M. N. G. (1979) *J. Mol. Biol.* **134,** 781–804.
26. James, M. N. G., Sielecki, A. R., Brayer, G. D., Delbaere, L. T. J. & Bauer, C.-A. (1980) *J. Mol. Biol.* **144,** 43–88.
27. Johnson, C. K. (1965) *ORTEP,* Report ORNL-3794 (Oak Ridge Natl. Lab., Oak Ridge, TN).
28. Bürgi, H. B., Dunitz, J. D. & Shefter, E. (1973) *J. Am. Chem. Soc.* **95,** 5065–5067.
29. Rossmann, M. G. & Argos, P. (1977) *J. Mol. Biol.* **109,** 99–129.
30. Deslongchamps, P. (1975) *Tetrahedron* **31,** 2463–2490.
31. Bizzozero, S. A. & Dutler, H. (1981) *Bioorg. Chem.* **10,** 46–62.
32. Bizzozero, S. A. & Zweifel, B. O. (1975) *FEBS Lett.* **59,** 105–108.